International Journal of Industrial Chemistry (IJIC)
a SpringerOpen Journal

RESEARCH Open Access

Carob seed oil: an efficient inhibitor of C38 steel corrosion in hydrochloric acid

Dris Ben Hmamou[1], Rachid Salghi[1*], Abdelkader Zarrouk[2], Omar Benali[3], Fatiha Fadel[2], Hassan Zarrok[4] and Belkheir Hammouti[2]

Abstract

Background: The carob seed oil (CO) was tested as inhibitor of the corrosion of C38 steel in 1 M HCl by weight loss and electrochemical measurements. The extract was found to inhibit the corrosion of C38 steel in 1 M HCl.

Results: The results of the study reveal that the inhibition efficiency of CO depends on its concentration and attains approximately 86.7% at 0.5 g/L. Polarization curves reveal that CO is a mixed-type inhibitor. Changes in impedance parameters (charge transfer resistance, R_t, and double-layer capacitance, C_{dl}) were indicative of CO adsorption on the metal surface, leading to the formation of a protective film. The effect of temperature on the corrosion behavior with the addition of 0.5 g/L of carob seed oil was studied in the temperature range of 298 to 328 K.

Conclusions: Results show that the inhibition efficiency of the plant extract increases with increasing temperature, and the adsorption of the latter on the C38 steel surface is found to obey the Langmuir adsorption isotherm. Some thermodynamic functions of dissolution processes were also determined.

Keywords: Carob seed oil, Inhibition, Corrosion, C38 steel, Adsorption

Background

Acid solutions generally used for the removal of rust and scale in industrial processes and the deterioration of metal due to these processes are very significant. Inhibitors are used in these processes to control metal dissolution. Hydrochloric acid is widely used in the pickling of steel and different steel-based alloys [1,2]. One way of protecting steel from corrosion is to use corrosion inhibitors. Organic compounds containing heteroatoms are commonly used to reduce the corrosion attack on steel in acidic media [3-16]. The recent trend is towards environmentally friendly inhibitors. Most of the natural products are non-toxic, biodegradable, and readily available in plenty. These advantages have incited us to draw a large part of our laboratory program to examine natural substances as corrosion inhibitors such as fennel oil [17], prickly pear seed oil [18], argan extract [18-21], argan oil [19,22], rosemary oil [23-25], *Thymus* oil [26,27], pennyroyal mint oil [28], lavender oil [29], jojoba oil [30], and *Artemisia* [31-33].

Carob fruits are among the most import tree fruit crops in the Mediterranean countries, and their production and consumption have increased considerably in recent years. They are widely used in the boiled juice 'pekmez' production and powder drink industry. The seeds of the carob are utilized in the food industry for their gum content [34]. The present work was established to study the corrosion inhibition of C38 steel in 1 M HCl solution by carob seed oil as corrosion inhibitor using different techniques: weight loss, potentiodynamic polarization, and electrochemical impedance spectroscopy (EIS).

Methods

Fatty acid composition

The fatty acid composition was determined following the ISO standard ISO 5509:2000 (ISO 2000) [35]. In brief, one drop of the oil was dissolved in 1 mL of n-heptane, 50 μg of sodium methylate was added, and the closed tube was agitated vigorously for 1 min at room temperature. After adding 100 μL of water, the tube was

* Correspondence: r_salghi@yahoo.fr
[1]Equipe de Génie de l'Environnement et de Biotechnologie, ENSA, Université Ibn Zohr, BP 1136, Agadir 8000, Morocco
Full list of author information is available at the end of the article

centrifuged at 4,500×*g* for 10 min, and the lower aqueous phase was removed. Then, 50 μL of HCl (1 mol with methyl orange) was added, the solution was shortly mixed, and the lower aqueous phase was rejected. About 20 mg of sodium hydrogen sulfate (monohydrate, extra pure; Merck, Darmstadt, Germany) was added, and after centrifugation at 4,500×*g* for 10 min, the top n-heptane phase was transferred to a vial and injected in an Agilent Technologies 6890 N gas chromatograph equipped with a capillary column (30 m × 0.32 mm; Supelco, Bellefonte, PA, USA) and flame ionization detection. The column was programmed to increase from 135°C to 160°C at 2°C/min and from 160°C to 205°C at 1.5°C/min; the detection temperature was maintained at 220°C, injector temperature 220°C. The vector gas was helium at a pressure of 5,520 Pa. Peaks were identified by comparing retention times with those of standard fatty acid methyl esters.

Weight loss measurements

Coupons cut into 2 cm × 2 cm × 0.08 cm dimensions (having composition of 0.179% C, 0.165% Si, 0.439% Mn, 0.203% Cu, 0.034% S, and Fe balance) are used for weight loss measurements. Prior to all measurements, the exposed area was mechanically abraded with 180, 320, 800, and 1,200 grades of emery papers. The specimens are washed thoroughly with bidistilled water, degreased, and dried with ethanol. Gravimetric measurements are carried out in a double-walled glass cell equipped with a thermostated cooling condenser. The solution volume is 80 cm^3. The immersion time for the weight loss is 6 h at 298 K.

Electrochemical tests

The electrochemical study was carried out using a potentiostat PGZ100 piloted by Voltamaster software. This potentiostat is connected to a cell with three electrode thermostats with double wall (Tacussel Standard CEC/TH). A saturated calomel electrode and platinum electrode were used as reference and auxiliary electrodes, respectively. The material used for constructing the working electrode was the same with that used for the gravimetric measurements. The surface area exposed to the electrolyte is 0.04 cm^2.

Potentiodynamic polarization curves were plotted at a polarization scan rate of 0.5 mV/s. Before all experiments, the potential was stabilized at free potential during 30 min. The polarization curves are obtained from −800 to −400 mV at 298 K. The solution test is thereafter de-aerated by bubbling nitrogen. Gas bubbling is maintained prior and throughout the experiments. In order to investigate the effects of temperature and immersion time on the inhibitor performance, some tests were carried out in a temperature range of 298 to 328 K.

The EIS measurements are carried out with the electrochemical system (Tacussel), which included a digital potentiostat model Voltalab PGZ100 computer (Radiometer Analytical, Lyon, France) at E_{corr} after immersion in solution without bubbling. After the determination of steady-state current at a corrosion potential, sine wave voltage (10 mV) peak to peak at frequencies between 100 kHz and 10 mHz are superimposed on the rest potential. Computer programs automatically controlled the measurements performed at rest potentials after 0.5 h of exposure at 298 K. The impedance diagrams are given in the Nyquist representation. Experiments are repeated three times to ensure the reproducibility.

Inhibition efficiencies EI% were calculated as follows:

- For weight loss measurement:

$$\mathrm{EI\%} = \frac{W^0_{corr} - W_{corr}}{W^0_{corr}} \times 100 \quad (1)$$

where W^0_{corr} and W_{corr} are the corrosion rates of steel due to the dissolution in 1 M HCl in the absence and the presence of definite concentrations of the inhibitor, respectively.

- For impedance measurements:

$$\mathrm{EI\%} = \frac{R_t - R^0_t}{R_t} \times 100 \quad (2)$$

where R_t and R^0_t are the charge transfer resistance values with and without the inhibitor, respectively.

- For potentiodynamic polarization measurements:

$$\mathrm{EI\%} = \frac{I^0_{corr} - I_{corr}}{I^0_{corr}} \times 100 \quad (3)$$

where I^0_{corr} and I_{corr} are the corrosion current densities in the absence and the presence of the inhibitor.

Results and discussion

Fatty acid composition

Gas chromatography analysis of dried plant extract showed that the plant extract contains ten different fatty acid methyl esters (Table 1). The main constituents were linoleic acid (45.05%), oleic acid (33.66%), palmitic acid (14.84%), and stearic acid (3.50%).

From this table, it is evident that the carob seed oil could serve as an effective green corrosion inhibitor. It is interesting to see here that all the identified compounds

Table 1 Chemical composition of the carob seed oil

Fatty acid methyl ester	Percentage (%)
Myristic acid (C14:0)	0.09
Palmitic acid (C16:0)	14.84
Palmitoleic acid (C16:1)	0.36
Heptadecanoic acid (C17:0)	0.08
Stearic acid (C18:0)	3.50
Oleic acid (C18:1)	33.66
Linoleic acid (C18:2)	45.05
Linolenic acid (C18:3)	1.06
Arachidic acid (C20:0)	0.38
Gadoleic acid (C22:0)	0.34

from the plant extracts contained oxygen and/or *p*-electrons in their molecules.

It is a known fact that adsorption of the inhibitors is the main process affecting the corrosion rate of metals. Inhibition adsorption can affect the corrosion rate in two possible ways [36]. In the first way, inhibitors decrease the available reaction area through adsorption on the metal, which is called geometric blocking effect. In the second way, inhibitors modify the activation energy of the cathodic and/or anodic reactions occurring in the inhibitor-free metal in the course of the inhibited corrosion process, which is called energy effect [37].

Effect of concentration

Gravimetric measurements

Values of the inhibition efficiency and corrosion rate obtained from the weight loss measurements of C38 steel for different concentrations of carob seed oil in 1 M HCl at 298 K after 6 h of immersion are given in Table 2. This shows that the inhibition efficiency increases with the increasing inhibitor concentration. At this purpose, one observes that the optimum concentration of the inhibitor required to achieve efficiency is found to be 0.50 g/L (EI% = 81.6%). The inhibition of C38 steel corrosion by carob seed oil (CO) can be explained in terms of adsorption on the metal surface. This compound can be adsorbed on the metal surface by the interaction between the pairs of oxygen electrons and the insaturation of the inhibitor molecules and the metal surface. This process is facilitated by the presence of vacant orbitals of low energy in iron atom, as observed in the transition group metals [38].

Table 2 Corrosion rate of C38 steel in 1 M HCl

Concentration (g/L)	W_{corr} (mg/cm^2)	E_W (%)
Blank	1.26	-
0.02	0.60	52.4
0.10	0.49	61.1
0.25	0.34	73.0
0.50	0.23	81.7

With and without carob seed oil at various concentrations (W_{corr}) and the corresponding inhibition efficiency (E_W).

Electrochemical impedance spectroscopy measurements

The corrosion behavior of C38 steel in acidic solution in the presence of CO was investigated by EIS methods at 298 K. Nyquist plots obtained for frequencies ranging from 100 kHz to 10 mHz at open circuit potential for C38 steel in 1 M HCl in the presence of various concentrations of CO are shown in Figure 1. The impedance diagrams obtained are not perfect semicircles, and the difference was attributed to frequency dispersion [38]. The fact that impedance diagrams have a semicircular appearance shows that the corrosion of steel is controlled by a charge transfer process. The equivalent circuit model employed for this system is presented in Figure 2. The resistance R_s is the resistance of the solution; R_t reflects the charge transfer resistance, and C_{dl} is the double-layer capacitance.

Values of the charge transfer resistance R_t were obtained from these plots by determining the difference in the values of impedance at low and high frequencies as suggested by Tsuru and Haruyama [39]. Values of the double-layer capacitance C_{dl} were calculated from the frequency at which the impedance imaginary component -Zi is maximum using the equation:

$$f\left(-\mathrm{Zi}_{\max}\right) = \frac{1}{2\,\pi\,C_{dl}\,R_t} \tag{4}$$

Table 3 gives the values of the charge transfer resistance R_t, double-layer capacitance C_{dl}, and inhibition efficiency obtained from the above plots. It can be seen that the presence of carob seed oil enhances the values of R_t and reduces the C_{dl} values. The decrease in C_{dl}, which can result from a decrease in local dielectric constant and/or an increase in the thickness of the electric double layer [40], suggested that CO molecules function by adsorption at the metal/solution interface. Thus, the decrease in C_{dl} values and the increase in R_t values and consequently of the inhibition efficiency may be due to the gradual replacement of water molecules (volumes of the water molecules is 27.19 A$^{\circ 3}$) by the adsorption of the extract molecules on the metal surface, decreasing the extent of dissolution reaction [41,42].

Polarization measurements

Figure 3 shows the polarization curves of C38 steel in 1 M HCl and in the presence of different concentrations

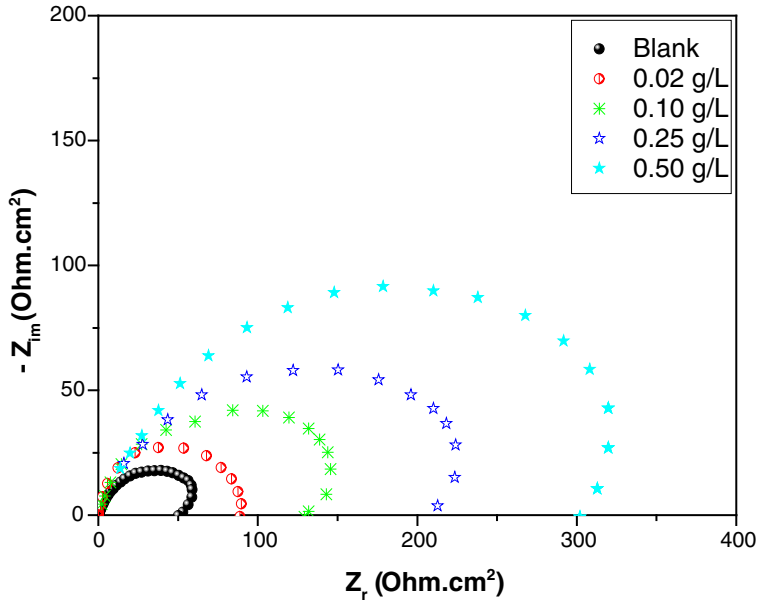

Figure 1 Nyquist diagrams for C38 steel electrode with and without carob seed oil. At E_{corr} after 30 min of immersion.

(0.02 to 0.5 g/L) of carob seed oil. With the increase of CO concentrations, both anodic and cathodic currents were inhibited. This result shows that the addition of CO reduces anodic dissolution and also retards the hydrogen evolution reaction.

Table 4 gives the values of kinetic corrosion parameters as the corrosion potential E_{corr}, corrosion current density I_{corr}, Tafel slope b_c, and inhibition efficiency for the corrosion of C38 steel in 1 M HCl with different concentrations of carob seed oil. The corrosion current densities were estimated by Tafel extrapolation of the cathodic curves to the open circuit corrosion potential. From Table 4, the following can be concluded:

- The I_{corr} values decrease with increasing inhibitor concentration.
- The addition of the carob seed oil produces slight changes in the values of E_{corr} and b_c. This indicates [43] that the adsorbed molecules of oil seed do not affect the mechanism of hydrogen evolution.

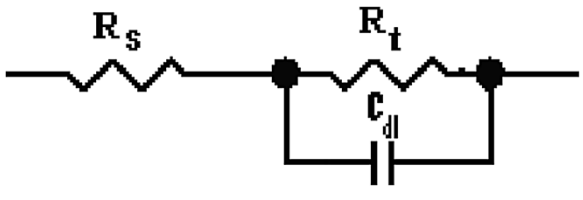

Figure 2 The electrochemical equivalent circuit used to fit the impedance spectra.

- The values of inhibition efficiency (EI%) increase with inhibitor concentration, reaching a maximum value (86.7%) at 0.5 g/L.

These polarization curve measurements were in good agreement with the corrosion weight loss and impedance tests.

Effect of temperature

To investigate the mechanism of inhibition and to calculate the activation energies of the corrosion process, EIS measurements were taken at various temperatures in the absence and presence of different concentrations of carob seed oil. Figures 4 and 5 give the Nyquist plots of C38 steel in the absence and presence of 0.5 g/L of carob seed oil at different temperatures.

Corresponding data are given in Table 5. In the studied temperature range (298 to 328 K), the values of R_t

Table 3 Impedance parameters for corrosion of C38 steel in 1 M HCl

Concentration (g/L)	R_t (Ωcm²)	f_{max} (Hz)	C_{dl} (μF/cm²)	EI (%)
Blank	48	50	66.3	-
0.02	90	62	11.99	46.6
0.10	125	75	9.91	61.6
0.25	214	91	8.17	77.5
0.50	300	100	5.30	84.0

In the absence and presence of different concentrations of carob seed oil at 298 K. C_{dl}, double-layer capacitance; EI, inhibitor efficiency; f_{max}, frequency at which the impedance imaginary component -Zi is maximum; R_t, charge transfer resistance.

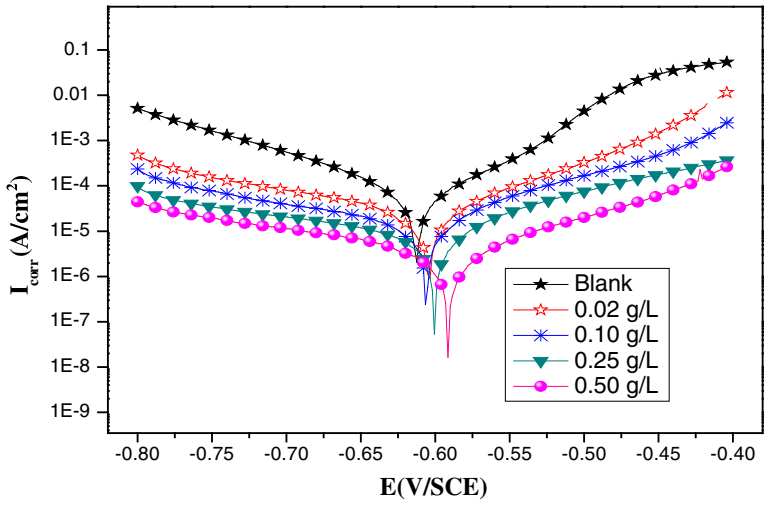

Figure 3 Potentiodynamic polarization curves of C38 steel in 1 M HCl. In the presence of different concentrations of carob seed oil.

decrease with increasing temperature both in uninhibited and inhibited solutions, and the values of the inhibition efficiency of carob seed oil increase with increasing temperature. The corrosion current density of C38 steel decreases more rapidly with temperature in the absence of the inhibitor; these results confirm that the plant extract acts as an efficient inhibitor in the temperature range studied.

The activation parameters for the corrosion process were calculated from Arrhenius-type plot according to the following equation:

$$\log I = -\frac{E_a}{2.303\,R\,T} + \log A \qquad (5)$$

where E_a is the apparent activation energy, A is the pre-exponential factor, R is the universal gas constant, and T is the absolute temperature.

The variations of the $1/R_t$ logarithm of C38 steel in HCl containing 0.5 g/L of carob seed oil used with the reciprocal of the absolute temperature are presented in Figure 6. Straight lines with coefficients of correlation higher than 0.99 are obtained.

Table 4 Electrochemical parameters of C38 steel in 1 M HCl solution

Concentration (g/L)	E_{corr} (mV/SCE)	I_{corr} (μA/cm^2)	$-b_c$ (mV/dec)	EI (%)
Blank	−612	124	149	-
0.02	−604	62	153	50.0
0.10	−606	39	158	68.0
0.25	−601	33	157	73.2
0.50	−592	16	155	86.7

With and without the carob seed oil at different concentrations. b_c, Tafel slope; E_{corr}, corrosion potential; EI, inhibitor efficiency; I_{corr}, corrosion current density.

Kinetic parameters such as enthalpy and entropy of the corrosion process may be evaluated from the temperature effect. An alternative formulation of Arrhenius equation is [44-46].

$$W = \frac{RT}{Nh}\exp\left(\frac{\Delta S_a^o}{R}\right)\exp\left(-\frac{\Delta H_a^o}{RT}\right) \qquad (6)$$

where h is Plank's constant, N is Avogrado's number, and ΔS°_a and ΔH°_a are the entropy and enthalpy of activation, respectively.

Straight lines are obtained with a slope ($-\Delta H^\circ_a/R$) and intercept (Ln $R/Nh + \Delta S^\circ_a/R$), from which the ΔH°_a and ΔS°_a values are calculated (Table 6 and Figure 7). The positive sign of the enthalpy (ΔH°_a) reflects the endothermic nature of the steel dissolution process. The entropy of activation ΔS°_a in the absence of the inhibitor is positive, and this value increases positively with the CO concentration. The increase of ΔS°_a implies that an increase in disordering takes place in going from the reactants to the activated complex [47].

The linear regression coefficients are close to one, indicating that the corrosion of C38 steel in 1 M HCl solution may be elucidated using the kinetic model. A close inspection of the data in Table 6 shows that the activation energy is lower in the presence of carob seed oil. The decrease of E_a is typical of the chemisorption process [15]. According to Equation 5, low values of A and high values of E_a lead to lower corrosion rates.

Adsorption isotherm and mechanism of inhibition

Adsorption isotherms are very important to understand the mechanism of corrosion inhibition reactions. The most frequently used isotherms are the Langmuir [48],

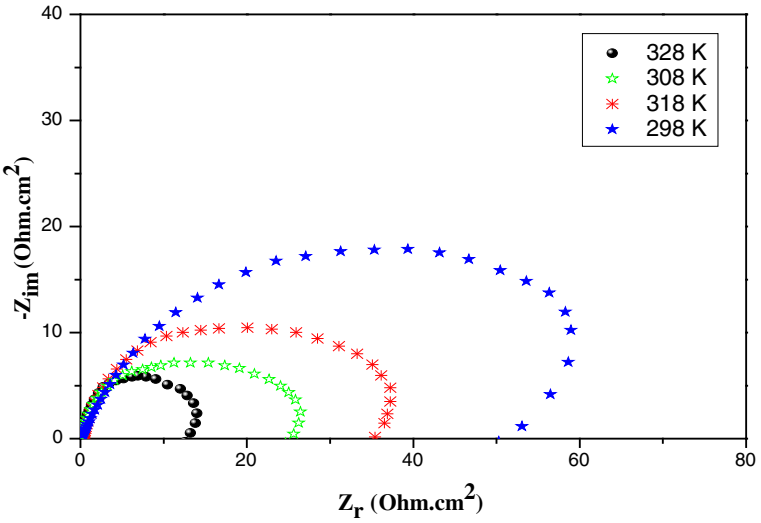

Figure 4 Nyquist diagrams for C38 steel in 1 M HCl at different temperatures.

Frumkin [49], and Temkin [50]. The Langmuir isotherm (C/θ vs C) assumes that there is no interaction between the adsorbed molecules on the surface. The Frumkin adsorption isotherm (θ vs C) assumes that there is some interaction between the adsorbates, and the Temkin adsorption isotherm (θ vs lg$C$) represents the effect of multiple layer coverage [51]. Figure 8 shows the dependence of C/θ as a function of the of CO concentration. The curve obtained clearly showing that the data fit well with the Langmuir adsorption isotherm was found to be the best description of the adsorption behavior of the studied inhibitor, which obeys:

$$\frac{C}{\theta} = \frac{1}{K} + C \qquad (7)$$

where C is the concentration of the inhibitor, K is the equilibrium constant of the adsorption process, and θ is the surface coverage.

This suggests that extract in present study obeyed the Langmuir isotherm and there is negligible interaction between the adsorbed molecules.

For the mechanism of adsorption, from the literature and in hydrochloric acid solution, the following mechanism is proposed for the corrosion of C38 steel [52,53].

The anodic dissolution mechanism of mild steel is as follows:

$$\mathrm{Fe} + \mathrm{Cl}^- \leftrightarrow (\mathrm{FeCl}^-)_{\mathrm{ads}},$$
$$(\mathrm{FeCl}^-)_{\mathrm{ads}} \leftrightarrow (\mathrm{FeCl}^+)_{\mathrm{ads}} + \mathrm{e}-,$$
$$(\mathrm{FeCl}^+) \leftrightarrow \mathrm{Fe}^{2+} + \mathrm{Cl}^-.$$

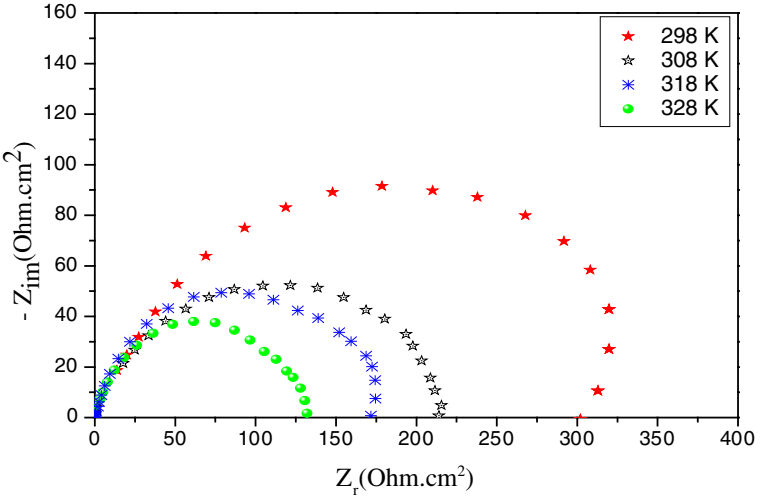

Figure 5 Nyquist diagrams for C38 steel in 1 M HCl + 0.5 g/L carob seed oil at different temperatures.

Table 5 Thermodynamic parameters for the adsorption of carob seed oil on the C38 steel

	Temperature (K)	R_t (Ωcm^2)	f_{max} (Hz)	C_{dl} ($\mu F/cm^2$)	EI (%)
Blank	298	48	50	66.3	-
	308	30	79	67.1	-
	318	22	100	72.3	-
	328	12	125	106.1	-
Carob seed oil	298	300	100	5.30	84.0
	308	223	90	7.92	85.6
	318	171	83	11.21	87.1
	328	130	79	15.49	90.7

C_{dl}, double-layer capacitance; f_{max}, frequency at which the impedance imaginary component -Zi is maximum; EI, inhibitor efficiency; R_t, charge transfer resistance.

The cathodic hydrogen evolution mechanism is as follows:

$$Fe + H^+ \leftrightarrow (FeH^+)_{ads},$$
$$(FeH^+)_{ads} + e- \leftrightarrow (FeH)_{ads},$$
$$(FeH)_{ads} + H^+ + e- \leftrightarrow Fe + H_2.$$

Generally, the corrosion inhibition mechanism in an acid medium is adsorption of the inhibitor on the metal surface. The process of adsorption is influenced by different factors like the nature and charge of the metal, the chemical structure of the organic inhibitor, and the type of aggressive electrolyte [53].

Considering the inhomogeneous nature of metallic surfaces resulting from the existence of lattice defects and dislocations, a corroding metal surface is generally characterized by multiple adsorption sites having activation energies and heats of adsorption. Inhibitor molecules may thus be adsorbed more readily at surface active sites having suitable adsorption enthalpies. According to the detailed mechanism above, the displacement of some adsorbed Cl^- water molecules on the metal surface by the inhibitor species to yield the adsorbed intermediate $(FeCl^-)_{ads}$ reduces the amount of the species $(FeCl^+)_{ads}$ available for the rate-determining steps and consequently retards Fe anodic dissolution.

Table 6 The value of activation parameters E_a, ΔH_a, and ΔS_a for C38 steel in 1 M HCl

Inhibitor	E_a (kJ/mol)	ΔH_a (kJ/mol)	ΔS_a (J/mol)	$E_a - \Delta H_a$ (KJ/mol)
Blank	36.20	33.61	−164.35	2.59
carob seed oil	22.53	19.93	−225.29	2.60

In the absence and presence of 0.5 g/L of carob seed oil. E_a, apparent activation energy; ΔH_a, enthalpy of activation; ΔS_a, entropy of activation.

Experimental

Oil extraction

The carob seeds were collected from Talioune (Taroudant) in Morocco in the summer of 2011. The seeds were removed from the carob fruits, finally washed with water, and left to air dry for 4 days. The previously cleaned seeds were comminuted into pieces. The seed pieces were then stored in an air-tight container in a refrigerator (−20°C) prior to analysis. Carob seed oil was obtained by extraction of the meal with petroleum ether (50°C) in a soxhlet extractor for 12 h. After extraction of

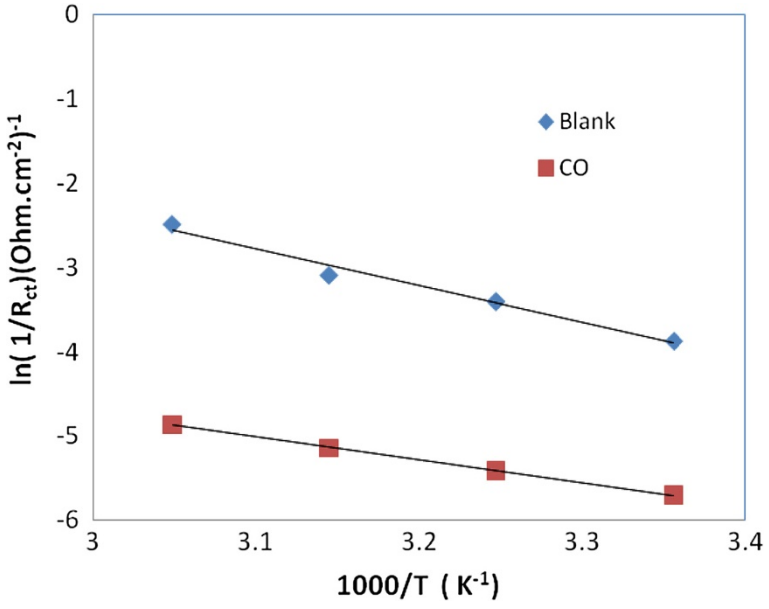

Figure 6 Arrhenius plots of C38 steel in 1 M HCl with and without 0.5 g/L carob seed oil.

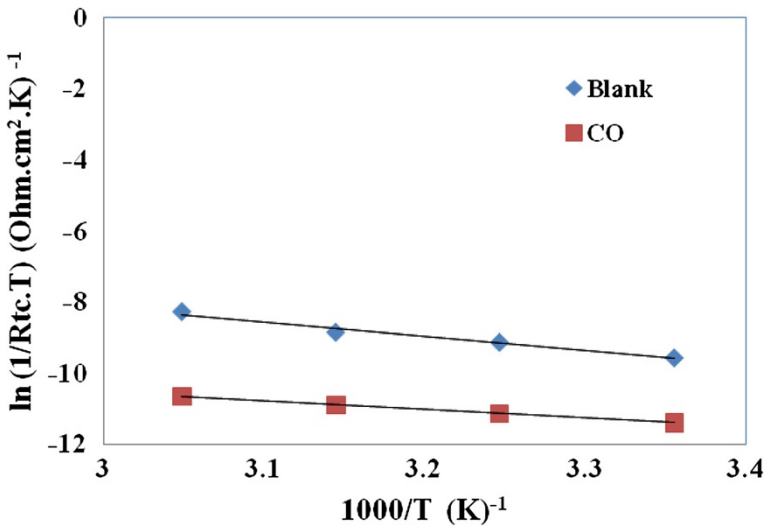

Figure 7 ln (1/*T*. R_t) vs 1/*T* of C38 steel in 1 M HCl. With and without 0.5 g/L carob seed oil.

the oil, the solvent was evaporated under reduced pressure. The obtained oil was kept in sealed glass bottles under deep-freezing (−18°C) for further analysis.

Solution preparation

The 1 M HCl solution was prepared by dilution of analytical-grade 37% HCl with double-distilled water. The test solutions were freshly prepared before each experiment by adding the oil directly to the corrosive solution. The test solution is thereafter de-aerated by bubbling nitrogen. Gas pebbling is maintained prior and throughout the experiments. The experiments were carried out in triplicate to ensure reproducibility.

Conclusions

Inhibitors play a vital role in providing protection against corrosion. The selection of the inhibitor is important for environmental protection. Not all inhibitors are eco-friendly.

There is a growing trend to use plant extracts and pharmaceutical compounds as corrosion inhibitors. Most of these compounds are environmentally friendly. Carob seed oil proved to be an eco-friendly inhibitor for C38 steel in 1 M HCl solution.

From the overall experimental results, the following conclusions can be deduced:

- Chemical analysis shows that the plant extract contains ten different fatty acid methyl esters.
- Carob seed oil mainly acts as a good inhibitor for the corrosion of C38 steel in 1 M HCl.
- Inhibition efficiency increases with both the concentration of the inhibitor and the temperature.

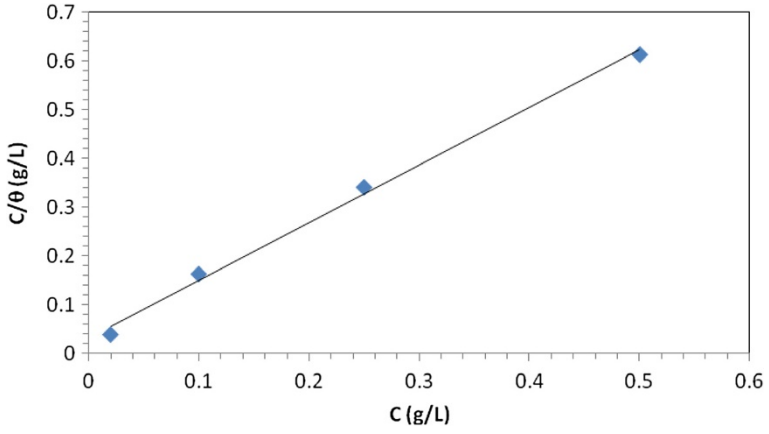

Figure 8 Langmuir adsorption isotherm of carob seed oil on the C38 steel surface by polarization measurements.

- The data obtained from the three different methods, potentiodynamic polarization, EIS, and weight loss, are in good agreement.
- The studied CO was adsorbed chemically on the steel surface according to the Langmuir isotherm model. Thermodynamic parameters are determined.

Competing interests
The authors declare that they have no competing interests.

Authors' contributions
OB carried out the data treatment and redaction of the manuscript. FF carried out the oil extraction and fatty acid composition. HZ carried out the gravimetric measurements. DBH and AZ studied the effect of temperature. RS and BH carried out the thermodynamic parameters and redaction of the manuscript. All authors read and approved the final manuscript.

Acknowledgements
The authors wish to thank the Volubilis MA/10/226 for supporting this work.

Author details
[1]Equipe de Génie de l'Environnement et de Biotechnologie, ENSA, Université Ibn Zohr, BP 1136, Agadir 8000, Morocco. [2]LCAE-URAC18, Faculté des Sciences, Université Mohammed Premier, BP 4808, Oujda 60000, Morocco. [3]Départment de Biologie, Faculté des Sciences et de la Technologie, Université Dr. Tahar, Moulay, Saïda 20000, Algeria. [4]Laboratoire des Procèdes de Séparation, Faculté des Sciences, Kénitra 14000, Morocco.

Received: 27 May 2012 Accepted: 20 September 2012
Published: 9 October 2012

References

1. Bentiss F, Gassama F, Barbry D, Gengembre L, Vezin H, Lagreneée M, Traisnel M (2006) Appl Surf Sci 252:2684
2. Khaled KF, Hackerma N (2003) Electrochim Acta 48:2715
3. Mihit M, El Issami S, Bouklah M, Bazzi L, Hammouti B, AitAddi E, Salghi R, Kertit S (2006) Appl Suf Sci 252:2389
4. Hammouti B, Salghi R, Kertit S (1998) J Electrochem Soc India 47:31
5. Zarrok H, Oudda H, Zarrouk A, Salghi R, Hammouti B, Bouachrine M (2011) Der Pharma Chemica 3:576
6. El Issami S, Bazzi L, Mihit M, Hilali M, Salghi R, El Ait A (2005) J Phys IV 123:307
7. El I, Bazzi L, Mihit M, Hammouti B, Kertit S, AitAddi E, Salghi R (2007) Pig Res Tech 36:161
8. Mihit M, Laarej K, Abou El Makarim H, Bazzi L, Salghi R, Hammouti B (2010) Arab J Chem 3:55
9. Mihit M, Salghi R, El Issami S, Bazzi L, Hammouti B, El Ait A, Kertit S (2006) Pig Res Tech 35:151
10. Barouni K, Bazzi L, Salghi R, Mihit M, Hammouti B, Albourine A, El Issami S (2008) Mater Lett 62:3325
11. El Issami S, Bazzi L, Hilali M, Salghi R, Kertit S (2002) Ann Chim Sci Mat 27:63
12. Salghi R, Bazzi L, Hammouti B, Kertit S (2000) Bull Electrochem 16:272
13. Benali O, Larabi L, Tabti B, Harek Y (2005) Anti-corr Meth Mater 52:280
14. Benali O, Larabi L, Mekelleche SM, Harek Y (2006) J Mater Sci 41:7064
15. Benali O, Larabi L, Harek Y (2009) J Appl Electrochem 39:769
16. Merah S, Larabi L, Benali O, Harek Y (2008) Pig Res Tech 37:291
17. Lahhit N, Bouyanzer A, Desjobert JM, Hammouti B, Salghi R, Costa J, Jama C, Bentiss F, Majidi L (2011) Port Electrochim Acta 29:127
18. Ben Hmamou D, Salghi R, Bazzi L, Hammouti B, Al-Deyab SS, Bammou L, Bazzi L, Bouyanzer A (2012) Int J Electrochem Sci 7:1303
19. Afia L, Salghi R, El B, Bazzi L, Errami M, Jbara O, Al-Deyab SS, Hammouti B (2011) Int J Electrochem Sci 6:5918
20. Afia L, Salghi R, Bammou L, Bazzi E, Hammouti B, Bazzi L (2012) Acta Metall Sin 25:10
21. Afia L, Salghi R, Bazzi E, Zarrouk A, Hammouti B, Bouri M, Zarrouk H, Bazzi L, Bammou L (2012) Res Chem Intermed. doi:10.1007/s11164-012-0496-y
22. Afia L, Salghi R, Bammou L, El B, Hammouti B, Bazzi L, Bouyanzer A (2011) J. Saudia Chem Soc. doi:10.1016/j.jscs.2011.05.008
23. Chetouani A, Hammouti B, Benkaddour M (2004) Res Pig Tech 33:26
24. El Ouariachi E, Paolini J, Bouklah M, Elidrissi A, Bouyanzer A, Hammouti B, Desjobert J-M (2010) J. Costa, Acta Metall Sin 23:13
25. Bendahou M, Benabdallah M, Hammouti B (2006) Pigm Res Techn 35:95
26. Bouyanzer A, Hammouti B (2004) Bull Electrochem 20:63
27. Bammou L, Chebli B, Salghi R, Bazzi L, Hammouti B, Mihit M, El Idrissi H (2010) Green Chem Lett Rev 3:173
28. Bouyanzer A, Hammouti B, Majidi L (2006) Mater Lett 60:2840
29. Zerga B, Sfaira M, Rais Z, Ebn Touhami M, Taleb M, Hammouti B, Imelouane B, Elbachiri A (2009) Mater. Tech 97:297
30. Bouyanzer A, Hammouti B (2004) Pigm. Resin Techn. 33:287
31. Benabdellah M, Hammouti B, Benkaddour M, Bendahhou M, Aouniti A (2006) Appl Surf Sci 252:6212
32. Bammou L, Mihit M, Salghi R, Bazzi L, Bouyanzer A, Hammouti B (2011) Int J Electrochem Sci 6:1454
33. Ouachikh O, Bouyanzer A, Bouklah M, Desjobert J-M, Costa J, Hammouti B, Majidi L (2009) Surf Rev Lett 6:49
34. Ozcan MM, Arslan D, Gokcalık H (2007) Int J Food Sci Nutr 58:652
35. International Standard ISO 5509 (2000) Animal and vegetable fats and oils - preparation of methyl esters of fatty acids, 2nd edition
36. Riggs OL, Jr (1973) In: Nathan CC (ed) Corrosion inhibitors, 2nd edition. Houston, NACE
37. Al-Otaibi MS, Al-Mayouf AM, Khan M, Mousa AA, Al-Mazroa SA, Alkhathlan HZ (2012) Arab. J. Chem.. doi:10.1016/j.arabjc.2012.01.015
38. Benali O, Larabi L, Traisnel M, Gengembre L, Harek Y (2007) Appl Surf Sci 253:6130
39. Tsuru T, Haruyama S, Gijutsu B (1978) J Jpn Soc Corros Eng 27:573
40. McCafferty E, Hackerman N (1972) J Electrochem Soc 119:146
41. Bentiss F, Traisnel M, Lagrenée M (2000) Corros Sci 42:127
42. Muralidharan S, Phani KLN, Pitchumani S, Ravichhandran S, Iyer SVK (1995) J Electrochem Soc 142:1478
43. Ateya BG, Abo El-Khair BM, Abdel Hamid IA (1976) Corros Sci 16:163
44. Benabdellah M, Tounsi A, Khaled KF, Hammouti B (2011) Arab J Chem 4:17
45. Elouali I, Hammouti B, Aouniti A, Ramli Y, Azougagh M, Essassi EM, Bouachrine M (2010) J Mater Environ Sci 1:1
46. Dahmani M, Et-Touhami A, Al-Deyab SS, Hammouti B, Bouyanzer A (2010) Int J Electrochem Sci 5:1060
47. Ouici HB, Benali O, Harek Y, Al-Deyab SS, Larabi L, Hammouti B (2012) Int J Electrochem Sci 7:2304
48. Langmuir I (1947) J Am Chem Soc 39:1848
49. Frumkin ANZ (1925) Phys Chem 116:466
50. De Boer JH (1968) The dynamical character of adsorption, 2nd edition. Claredon Press, Oxford, UK
51. Masel RI (1996) Principles of adsorption and reaction on solid surfaces. Wiley, New York
52. Bavarian B, Yeob K, Reiner L (2003) Corrosion protection of steel rebar in concrete by migrating corrosion inhibitors. NACE, Corrosion, Houston
53. Shahid M (2011) Adv Nat Sci: Nanosci Nanotechnol 2:043001

doi:10.1186/2228-5547-3-25
Cite this article as: Hmamou *et al.*: **Carob seed oil: an efficient inhibitor of C38 steel corrosion in hydrochloric acid.** *International Journal of Industrial Chemistry* 2012 **3**:25.